Plasma Scale Lenth Effects on Protons Generated in Ultra Intense Laser Plasmas

O.Culfa,[1,2] G.J.Tallents,[2] M.E. Korkmaz,[1] A.K.Rossall,[2] E.Wagenaars,[2] C.P.Ridgers,[2] C.D.Murphy,[2] N.Booth,[3] D.C. Carroll,[3] L.A. Wilson,[3] K.L.Lancaster,[2,3] and N.C.Woolsey[2]

[1)] *Department of Phyics, Karamanoglu MehmetBey University, Karaman, TURKEY*

[2)] *York Plasma Institute, The Department of Physics, The University of York, York YO10 5DD, UK*

[3)] *CLF, STFC Rutherford Appleton Laboratory, Didcot, Oxfordshire OX11 0QX, UK*

(Dated: 30 August 2016)

The energy spectra of protons generated by ultra intense (10^{20} W cm^{-2}) laser interactions with a pre formed plasma of scale length measured by shadowgraphy are presented. The effects of the preformed plasma on the proton beam temperature and number of protons are evaluated. 2D EPOCH PIC code simulations of the proton spectra are found to be in agreement with measurements over a range of experimental parameters.

I. INTRODUCTION

High power lasers are enabling the irradiation of solid targets at irradiances exceeding 10^{18} W cm^{-2} with consequent production of high energy electrons, ions and x-rays. Experiments have demonstrated intense bursts of ions emitted from the rear of targets (the non-irradiated side) with energies up to several tens of mega-electron volts[1,2] with the acceleration produced by the production of an electric potential sheath associated with fast electrons penetrating through the target. The planar nature of targets enables an approximately one-dimensional acceleration of ions with the process referred to as target normal sheath acceleration (TNSA). Protons arising from impurity hydrogen on the back surface of the targets are preferentially accelerated due to their high charge to mass ratio compared to other ions and their abundance in typical targets at the surface.

The physics of TNSA as an explanation of energetic protons emitted from the back of solid targets during Petawatt laser irradiation was first presented by Wilks et al[3]. More recent results have been reviewed by Roth and Schollmeier[4]. The irradiance of 10^{18} W cm^{-2} for laser light of wavelength λ around one micron represents the threshold for the $\mathbf{J} \times \mathbf{B}$ electron acceleration process to become significant. In $\mathbf{J} \times \mathbf{B}$ acceleration, electrons are accelerated in the direction of the laser **k**-vector due to a $\mathbf{J} \times \mathbf{B}$ force arising from a transverse current $\mathbf{J} = n_e e \mathbf{E}$, where $\mathbf{E}$ and $\mathbf{B}$ are the laser electric and magnetic fields respectively (and n_e is the electron density). The $\mathbf{J} \times \mathbf{B}$ acceleration starts to dominate at irradiances $> 10^{18}$ W cm^{-2} where the ponderomotive potential ($e^2 E_o^2/4m\omega^2$ with $\omega = 2\pi c/\lambda$) exceeds the electron rest mass energy (mc^2). At irradiances $> 10^{18}$ W cm^{-2} , electrons are accelerated to relativistic velocities into the target. Due to the low cross-section for relativistic electron collisions with atoms, the electrons pass through even thick (> 10 μm) targets, with current flow limited by the Alfven limit as moderated by a return current from back to front of the target. Alfven showed that the limiting factor for the propagation of an electron beam is the self-generated magnetic beam, which bends the electrons back toward their source[5]. A return current in the irradiated target area enables the Alfven limit for the electron flux to be exceeded and a potential in electron volts at the back of the target of value equal to the hot electron temperature T_e in electron volts to be formed[3].

The propagation and application of laser accelerated electrons passing through the solid target is a subject of on-going research. For example, there is evidence associated with hollow ion emission for the creation of intense radiation fields equivalent to keV blackbody intensities due to electrons undergoing bremsstrahlung and Thomson scattering as they propagate through the target[6,7]. In hollow ion, two or more bound electrons are removed from an atomic inner shell giving rise to uniquely identifiable spectral lines. Such double ionisation from an inner shell can only be produced by an intense radiation field as Auger processes quickly fill vacant inner-shell quantum states and, if significant, collisional ionization is closely balanced by collisional three-body recombination.

Experimental parameter studies showing the effects of target thickness and the plasma scale-length at the front of the target are useful in elucidating understanding and in the development of applications of laser-accelerated protons arising from the back of the target. We present measurements of the energies of protons accelerated from the rear of targets along the target normal in ultra-intense irradiation at 10^{20} W cm^{-2}. We have deliberately used a pre-pulse to irradiate the target before the high power laser irradiation in order to establish a plasma of controlled scale-length into which the high power laser interacts. The scale-length of the plasma formed by the pre-pulse at the time of the high power laser irradiance is measured using transverse probe shadowgraphy. Electron energy and temperature measurements with the controlled density scale-length have been reported by Culfa et al[8,9]. This paper investigates the effects of the electrons accelerated through the target on the TNSA of protons measured along the target normal at the back of the target. We present ion spectra and fitted temperatures as a function of the plasma density scale-length and target thickness. Our experimental measurements are consistent with two dimensional particle-in-cell (PiC) code simulations also presented.

II. EXPERIMENTAL SETUP

The Vulcan laser system at the Rutherford Appleton Laboratory (RAL) has been utilised for the measurement of proton energies. The petawatt laser delivers 1.054 μm wavelength laser pulses of $\sim$ 1ps duration and pulse energies 150 $\pm$ 20 J with an intensity contrast of 10^8. Laser irradiance of 10^{20} W cm^{-2} in a p-polarized beam was incident at 40° angle to a plane target normal. A 5 ns duration pre-pulse was incident at 17° incidence angle with peak irradiance 1.5 ns prior to the main pulse. The petawatt laser was focussed onto plane foil of parylene-N (CH) in various thicknesses from 6 μm to 150 μm. The targets contained a thin (100nm) layer of aluminium buried at depths $\geq 3\ \mu$m from the target surface. The experiment set up is schematically illustrated in figure 1.

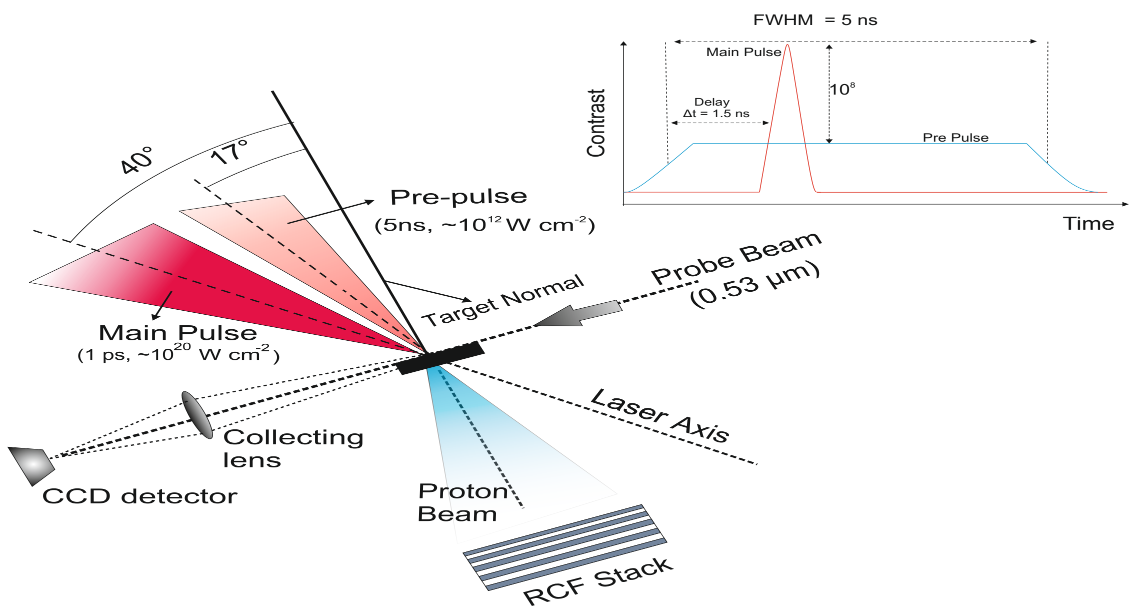

FIG. 1. Experimental setup in the Vulcan Petawatt Laser Facility for the measurement of proton energy along the target normal and density gradients normal to the target surface. The inset shows the timing of a pre pulse used to modify the interaction density scale length.

A frequency doubled optical probe beam was used to record the expanding density profile of the plasma at the time of the interaction pulse. The probe beam was directed parallel to the target surface passing through the plasma produced by the longer pulse laser target interaction. In our previous work[9], we have discussed in detail how to measure and analyse plasma density scale length from the shadowgraphy images obtained using the optical probe.

The distrubiton of multi-MeV protons along the target normal from the rear of the target were measured as a function of energy using passive stacks of dosimetry radiochromic film (RCF)[10], which were located 5 cm from the rear of the target and centered on the target normal axis. Number, energy and fitted temperature of accelerated protons were measured as a function of target thickness and the plasma scale length which varies with the pre-pulse intensity[8].

III. EXPERIMENTAL RESULTS

Proton numbers as a function of energy have been deduced from stacked RCF (Gafchromic HDF-810) exposure. A 10 μm thick aluminium foil acts to block scattered laser light and all plasma thermal emission expected from the back of the target (photon energies < 1 keV). The electron flux of energy up to 200 MeV is directed parallel to the laser axis at 40° to the target normal[9] and is not directed at the RCF stack. Protons are attenuated in the RCF stack of radiochromic films as they transmit through the different films and interspersed filters, with the exposure of the films giving the flux of protons of energy sufficient to penetrate through the overlay films and filters. Each film exposes predominantly at a particular proton energy due to the Bragg peak nature of proton absorption in matter. The background angle independent exposure of the RCF film includes exposure due to hard x-ray emission (> 1 keV) and is subtracted from exposure measurements. More details of the RCF measurements of proton energies and the method of analysis is given by Schollmeier et al[11].

Proton numbers recorded from the back of the target were found to peak on the target normal axis consistent with TNSA acceleration. The log-linear nature of the proton energy spectra allows a deduction of a proton temperature (kT_p) by fitting the proton spectra with variations of form $\exp(-E/kT_p)$. The variation of the fitted temperatures with the target thickness and the measured front surface density scalelength are shown in figures 2 and 3 respectively.

The total number N_T of protons can be evaluated from the proton energy spectra using the spectrum number in MeV extrapolated to zero energy ($n(0)$) and multiplying by the deduced proton temperature. We can write that

$$N_T = \int_0^\infty n(0)\mathrm{exp}\left(\frac{-E}{kT_p}\right) dE \quad = n(0)kT_p. \tag{1}$$

The number of fast electrons increases with the density scale length[8] and this results in a larger number of protons with increasing scale length (figure 4) .

.

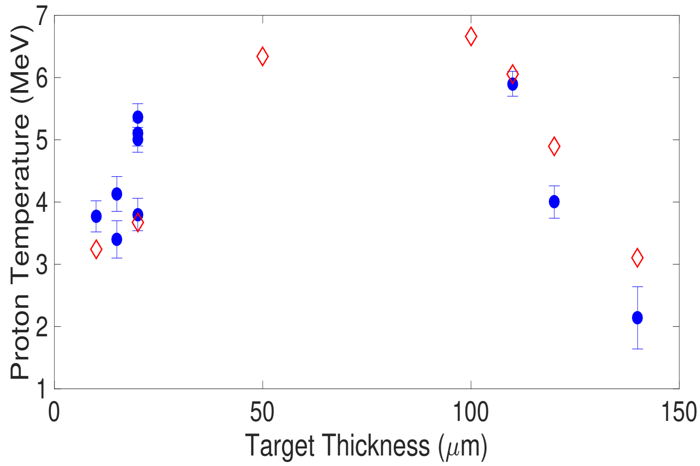

FIG. 2. Experimental and simulated measurements of proton temperature as a function of the target thickness for a number of individual laser shots. The plasma density scale length measured experimentally and used in the simulation was fixed at 0.5 μm. Red diamonds represents the PIC code simulations and blue circles are experimental data

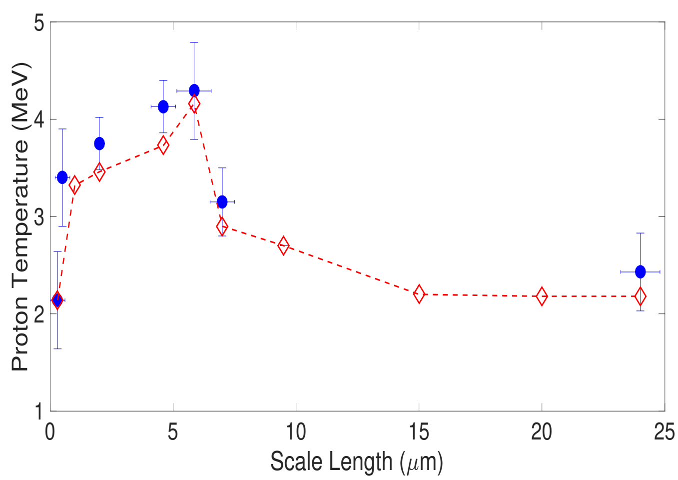

FIG. 3. Experimental measurements of proton temperature as a function of the measured plasma density scale length for a number of individual laser shots (circles) with target thichness of 20 μm. Superimposed are 2D PIC code simulations (red diamonds) with the preformed scale length and experimental parameters of the experiment.

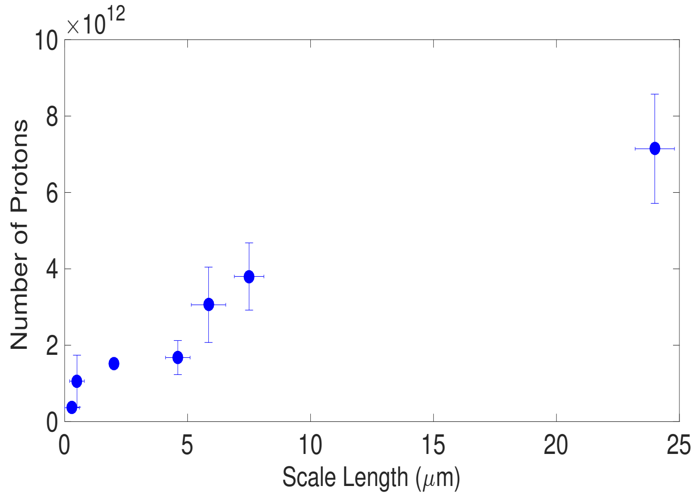

FIG. 4. Experimental measurements of number of protons as a function of the measured plasma scale length for a number of individual laser shots.

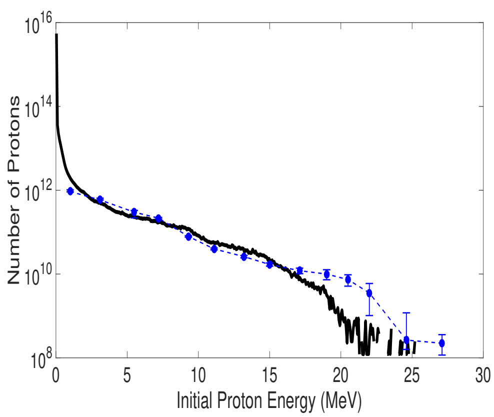

(a)

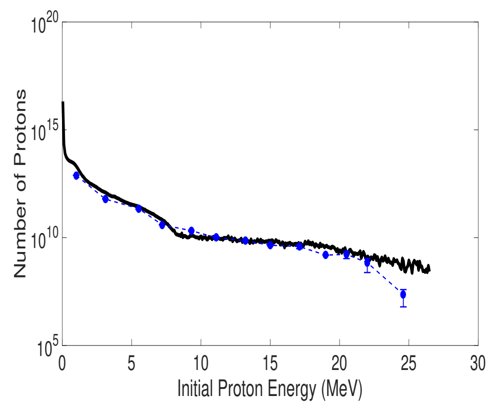

(b)

FIG. 5. Comparison of EPOCH 2D PIC code results with experimental proton spectra for a) 20 μm , b) 120 μm target thickness. The continuous black line represents the simulation results, while the blue dotted points are the experimental data. The absolute values of vertical scales are arbitrary and the experimental and simulated spectra are visually superimposed to match vertically.

IV. COMPARISON OF EPOCH 2D PIC CODE SIMULATIONS WITH EXPERIMENTALLY MEASURED PROTON SPECTRA

The 2D PIC code EPOCH[12] was used to simulate the experimental proton spectra for different target thicknesses and plasma density scale length. The system size was 90 μm $\times$ 90 μm with a mesh resolution of 1000 $\times$ 1000 cells with 48 particles of electrons and protons in a cell. The experimental variation of proton energy spectra for different target

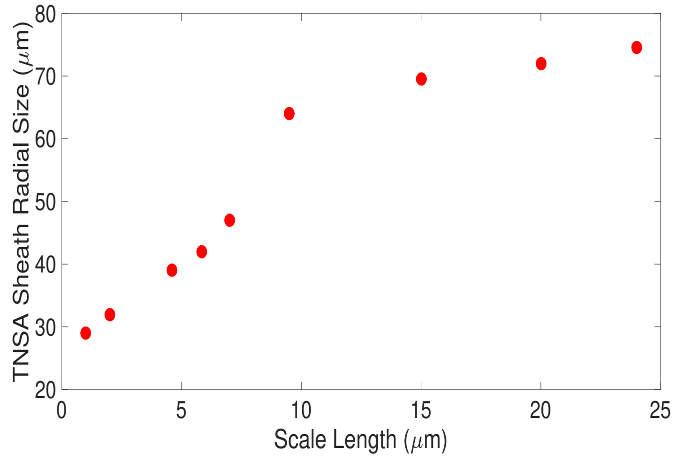

FIG. 6. Simulation results for TNSA sheath field measurements as a function of the plasma scale length.

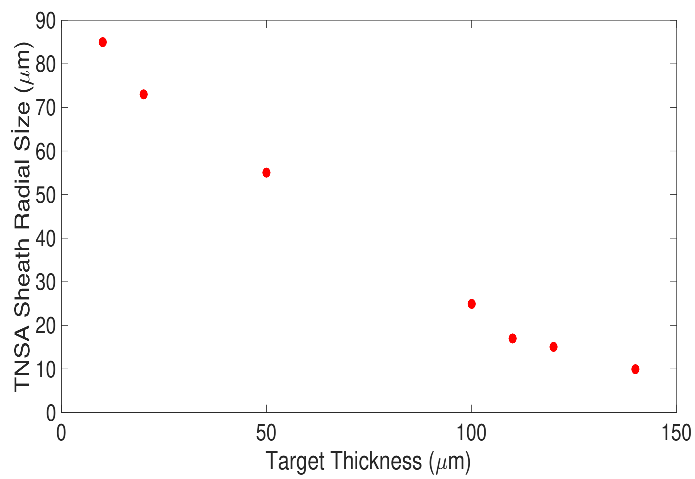

FIG. 7. Measured TNSA sheath field distance obtained by EPOCH 2D PIC simulations as a function of the target thickness

thicknesses with the laser irradiance of 3.5×10^{20} W cm^{-2} focussed on a 7 μm focal spot with an incidence angle of 40° degrees was determined. The laser wavelength and pulse duration were 1μm and 1 ps, respectively. In the simulations, the peak electron density was limited at 50 n_c where n_c is the critical density. A constant exponential density profile was assumed with the scale lengths L in the range of 0.5 μm to 25 μm.

The proton energy spectra was extracted at time 0.5 ps. Figure 5 compares the generated proton spectra from the 2D PIC code to the experimental proton energy spectra for different target thicknesses. The continuous line represent the EPOCH 2D PIC code simulation results and red dotted line with diamonds shows our experimental observations.

In order to understand the increase in the number of protons with increasing scale length with a constant target thickness block (20μm thick) have measured the TNSA sheath field with varying scale length and target thickness (figures 6 and 7).

Experimentally measured and simulated results of proton temperature as a function of the target thickness can be seen in figure 2 and as a function of plasma scale length in figure 3. Blue circles represents the experimental results while red diamons represent PIC simulations. Experimental and simulations results show that peak proton temperature occurs for target thickness around 50 μm and density scale lengths around 5 μm.

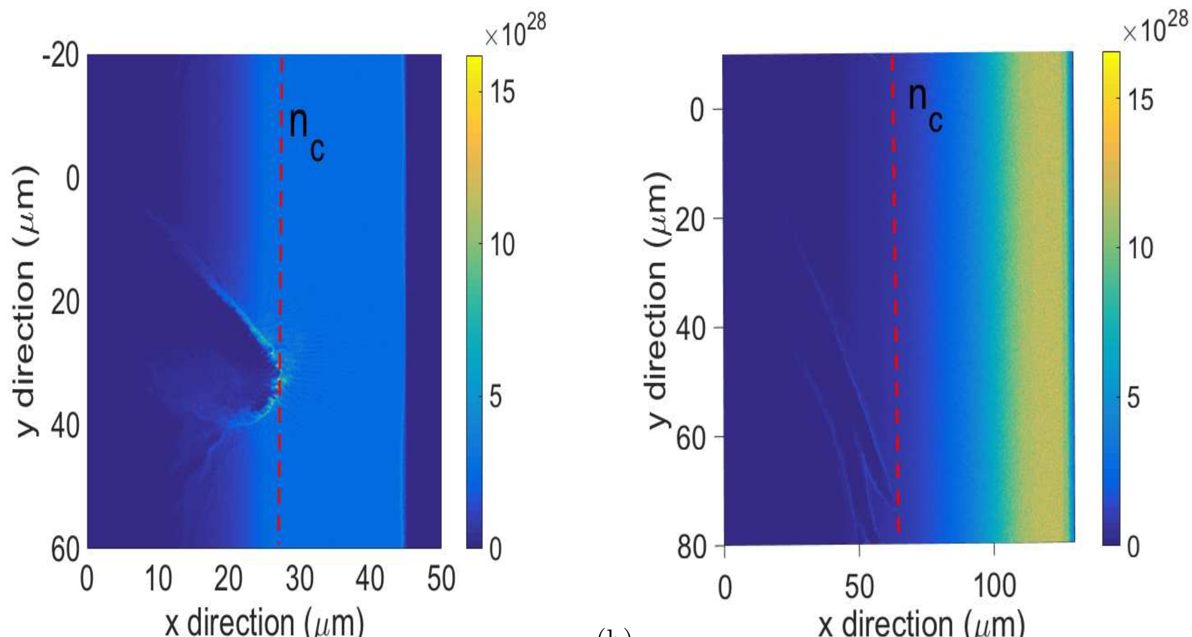

(a) (b)

FIG. 8. An example of electron density values colour-coded in units of m^{-3} after 0.55 ps with a) 5 μm , b) 15 μm scale length as simulated by the EPOCH 2D PIC code. The dashed vertical line indicates the critical density surface. The laser radiation is incident at 40° to the target normal.

At the high irradiances (10^{20} W cm^{-2}) of our experiment, electrons are expelled from the laser propagation axis due to the ponderomotive force. The plasma refractive index on axis is increased due to the electron density drop which produces a positive lensing effect[13]. Laser pulses also undergo self-focusing due to relativistic mass increase of the electrons accelerated by high irradiance laser light[14]. The transverse ponderomotive force can be sufficiently large to expel a significant fraction of the electrons from the high intensity laser region, creating ion channels (see figure 8). With the longer plasma propagation distances associated with longer plasma scalelengths, the laser pulse can be subject to transverse instabilities, resulting in beam filamentation. The filamentation reduces the local laser irradiance and reduces the temperature of accelerated electrons[9]. The drop at electron temperature reduces the generated proton temperature as well at the longer scale lengths. The measured proton temperatures vary with plasma scale length (figure 3) following the electron temperature which show a peak at scale lengths of 7.5 μm (see Culfa et al.[9]).

V. CONCLUSION

We have presented measurements of number, energy and temperature of protons in high irradiance laser plasma interactions with a preformed plasma of measured density scale length. The experimentally observed proton temperatures decreases for longer scale lengths as predicted by a 2D PIC code. Our experimental and simulation parameter studies of proton energies from high irradiance laser plasmas show that the 2D PIC code simulations are accurate and will help in the development of applications for laser accelerated protons.

VI. ACKNOWLEDGEMENTS

The authors gratefully acknowledge the assistance of laser operations, target preparation and engineering staff at the Central Laser Facility of RAL. Part of the research was supported by RFBR research project # 15-32-21121 and RAS Presidium Program for Basic Research # 13. This work was in part funded by the UK EPSRC grants EP/G054950/1, EP/G056803/1, EP/G055165/1 and EP/ M022463/1.

REFERENCES

[1]H. Daido, M. Nishiuchi, and A.S. Pirozhkov. *Rep.Prog.Phys.*, 75(056401), 2012.

[2]A. Macchi, M. Borghesi, and M. Passoni. *Rev. Mod. Phys.*, 85:751–793, 2013.

[3]S.C. Wilks, A.B. Langdon, T.E. Cowan, M. Rooth, M. Singh, S. Hatchett, M.H. Key, D. Pennington, A. MacKinnon, and R.A. Snavely. *Physics of Plasmas*, 8(542), 2001.

[4]M.ROTH and M. SCHOLLMEIER. *CERN Yellow Reports*, 1:231, 2016.

[5]H.Alven. *Phys.Rev.*, 55:425, 1939.

[6]. J. Colgan, J. Abdallah Jr., A. Ya. Faenov, S. A. Pikuz, E. Wagenaars, N. Booth, O. Culfa, R. J. Dance, R. G. Evans, R. J. Gray, T. Kaempfer, K. L. Lancaster, P. McKenna, A. L. Rossall, I. Yu. Skobelev, K. S. Schulze, I. Uschmann, A. G. Zhidkov, and N. C. Woolsey. *Phys.Rev.Lett.*, 110:125001, 2013.

[7]S. B. Hansen, J. Colgan, A. Ya. Faenov, J. Abdallah Jr., S. A. Pikuz, I. Yu. Skobelev, E. Wagenaars, N. Booth, O. Culfa, R. J. Dance, G. J. Tallents, R. G. Evans, R. J. Gray, T. Kaempfer, K. L. Lancaster, P. McKenna, A. K. Rossall, K. S. Schulze, I. Uschmann, A. G. Zhidkov, and N. C. Woolsey. *Phys.Plasmas.*, 21:031213, 2013.

[8]O. Culfa, G. J. Tallents, E. Wagenaars, C. P. Ridgers, R. J. Dance, A. K. Rossall, R. J. Gray, P. McKenna, C. D. R. Brown, S. F. James, D. J. Hoarty, N. Booth, A. P. L. Robinson, K. L. Lancaster, S. A. Pikuz, A. Ya. Faenov, T. Kampfer, K. S. Schulze, I. Uschmann, and N. C. Woolsey. *Phys.Plasmas*, 21:043106, 2014.

[9]O. Culfa, G. J. Tallents, A. K. Rossall, E. Wagenaars, C. P. Ridgers, C.D. Murphy, R. J. Dance, R. J. Gray, P. McKenna, C. D. R. Brown, S. F. James, D. J. Hoarty, N. Booth, A. P. L. Robinson, K. L. Lancaster, S. A. Pikuz, A. Ya. Faenov, T. Kampfer, K. S. Schulze, I. Uschmann, and N. C. Woolsey. *Phys.Rev.E*, 93:043201, 2016.

[10]F. Nurnberg, M. Schollmeier, E. Brambrink, A. Blazevic, D. C. Carroll, K. Flippo, D. C. Gautier, M. Geibel, K. Harres, B. M. Hegelich, O. Lundh, K. Markey, P. McKenna, D. Neely, J. Schreiber, and M. Roth. *Rev.Sci.Inst.*, 80:033301, 2009.

[11]M. Schollmeier, M. Geissel, A. B. Sefkow, and K. A. Flippo. *Rev.Sci.Inst.*, 85:043305, 2014.

[12]T D Arber, K Bennett, C S Brady, A Lawrence-Douglas, M G Ramsay, N J Sircombe, P Gillies, R G Evans, H Schmitz, A R Bell, and C P Ridgers. *Plasma Physics and Controlled Fusion*, 57(11):1–26, 2015.

[13]C. Max, J. Arons, and A.B. Langdon. *Phys.Rev.Lett*, 33:209, 1974.

[14]N. Naseri, S. G. Bochkarev, and W. Rozmus. *Phys.Plasmas*, 17:033107, 2010.